

Chronic mirabegron treatment increases human brown fat, HDL cholesterol, and insulin sensitivity

Alana E. O'Mara, ... , Kong Y. Chen, Aaron M. Cypess

J Clin Invest. 2020. <https://doi.org/10.1172/JCI131126>.

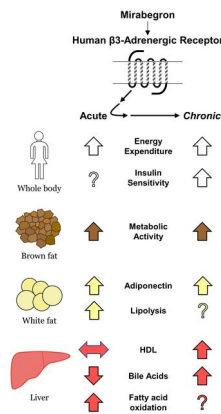
Clinical Research and Public Health

In-Press Preview

Endocrinology

Metabolism

Graphical abstract



Find the latest version:

<https://jci.me/131126/pdf>



**Chronic mirabegron treatment increases
human brown fat, HDL cholesterol, and insulin sensitivity**

Alana E. O'Mara,^{1,8} James W. Johnson,^{1,8} Joyce D. Linderman,¹ Robert J. Brychta,¹ Suzanne
McGehee,¹ Laura A. Fletcher,¹ Yael A. Fink,¹ Devika Kapuria,² Thomas M. Cassimatis,¹ Nathan
Kelsey,¹ Cheryl Cero,¹ Zahraa Abdul-Sater,¹ Francesca Piccinini,³ Alison S. Baskin,¹ Brooks P.
Leitner,¹ Hongyi Cai,⁴ Corina M. Millo,⁵ William Dieckmann,⁵ Mary Walter,⁶ Norman B. Javitt,⁷
Yaron Rotman,² Peter J. Walter,⁴ Marilyn Ader,³ Richard N. Bergman,³ Peter Herscovitch,⁵
Kong Y. Chen,¹ Aaron M. Cypess,^{1*}

¹Diabetes, Endocrinology, and Obesity Branch, Intramural Research Program, National
Institute of Diabetes and Digestive and Kidney Diseases, National Institutes of Health, Bethesda,
MD 20892, USA

²Liver Diseases Branch, National Institute of Diabetes and Digestive and Kidney Diseases,
National Institutes of Health, Bethesda, MD 20892, USA

³Diabetes and Obesity Research Institute, Cedars-Sinai Medical Center, Los Angeles, CA,
90048

⁴Clinical Mass Spectrometry Core, National Institute of Diabetes and Digestive and Kidney
Diseases, National Institutes of Health, Bethesda, MD 20892, USA

⁵Positron Emission Tomography Department, National Institutes of Health, Bethesda, MD
20892, USA.

⁶Clinical Laboratory Core, National Institute of Diabetes and Digestive Kidney Diseases,
National Institutes of Health, Bethesda, MD 20892, USA

⁷Departments of Medicine and Pediatrics, NYU School of Medicine, New York, NY 10016

⁸Shared contribution

Conflict of interest statement

The authors have declared that no conflict of interest exists,

Brief Summary: Treatment of healthy women with the β 3-adrenergic receptor agonist mirabegron for four weeks increased brown fat metabolic activity, HDL-cholesterol, tissue glucose uptake, and insulin sensitivity.

1 **ABSTRACT**

2 **Background.** Mirabegron is a β 3-adrenergic receptor (β 3-AR) agonist approved only for the
3 treatment of overactive bladder. Encouraging preclinical results suggest that β 3-AR agonists
4 could also improve obesity-related metabolic disease by increasing brown adipose tissue (BAT)
5 thermogenesis, white adipose tissue (WAT) lipolysis, and insulin sensitivity.

6 **Methods.** We treated 14 healthy women of diverse ethnicity, 27.5 ± 1.1 y, BMI 25.4 ± 1.2
7 kg/m^2 , with 100 mg mirabegron (Myrbetriq® extended-release tablet, Astellas Pharma) for four
8 weeks, open-label. The primary endpoint was the change in BAT metabolic activity as measured
9 by [^{18}F]-2-fluoro-D-2-deoxy-D-glucose (^{18}F -FDG) positron emission tomography/computed
10 tomography (PET/CT). Secondary endpoints included resting energy expenditure (REE), plasma
11 metabolites, and glucose and insulin metabolism as assessed by frequently sampled intravenous
12 glucose tolerance test.

13 **Results.** Chronic mirabegron therapy increased BAT metabolic activity. Whole-body REE was
14 higher, without changes in body weight or composition. Additionally, there were elevations in
15 plasma levels of the beneficial lipoprotein biomarkers high-density lipoprotein (HDL) and
16 ApoA1, as well as total bile acids. Adiponectin, a WAT-derived hormone that has anti-diabetic
17 and anti-inflammatory capabilities, increased with acute treatment and was 35% higher at study
18 completion. Finally, an intravenous glucose tolerance test demonstrated higher insulin
19 sensitivity, glucose effectiveness, and insulin secretion.

20 **Conclusion.** These findings indicate that human BAT metabolic activity can be increased after
21 chronic pharmacological stimulation with mirabegron and support the investigation of β 3-AR
22 agonists as a treatment for metabolic disease.

23 **Trial Registration:** Clinicaltrials.gov NCT03049462

24 **Funding.** This work was supported by the Intramural Research Program of the National
25 Institute of Diabetes and Digestive and Kidney Diseases (NIDDK), DK075112, DK075116,
26 DK071013, and DK071014.

27 **INTRODUCTION**

28 The rising rates of obesity are a global health epidemic. In the US alone, by 2030 it is
29 predicted that 86% of adults will be overweight or obese (1). Comorbidities include impaired
30 glucose tolerance, dyslipidemia, hypertension, and a proinflammatory state (2). Addressing
31 these problems with behavioral interventions alone has been largely unsuccessful, highlighting
32 the need in many patients for adjunct therapy to maintain long-term improvements in obesity-
33 related metabolic disease (3). One complementary approach has been pharmacological treatment
34 to increase fatty acid and glucose oxidation. For several decades, an attractive target has been
35 the β 3-adrenergic receptor (β 3-AR), whose activation in rodents leads to increased energy
36 expenditure and improved glucose tolerance (4). The mechanism has thought to include a
37 combination of increased brown adipose tissue (BAT) thermogenesis and white adipose tissue
38 (WAT) capacity for glucose uptake (4, 5).

39 Translation of the β 3-AR rodent studies to humans has not been straightforward. Species
40 differences in drug selectivity, oral bioavailability, and gene expression were limiting factors for
41 achieving weight loss (6, 7). Nevertheless, early-phase clinical trials showed improved glucose
42 tolerance (8) and increased fatty acid oxidation (9). Using the β 3-AR agonist mirabegron
43 (Myrbetriq®, extended-release tablet, Astellas Pharma), approved for the treatment of overactive
44 bladder, we recently showed that a single 200 mg dose stimulated BAT glucose uptake, WAT
45 lipolysis, and altered bile acid metabolism in healthy lean men (7). Neither the acute nor the
46 chronic effects of mirabegron on adult women have been examined, so the current study
47 addressed the hypothesis that four weeks of treatment with mirabegron could increase BAT
48 metabolic activity.

49 **RESULTS**

50 Fourteen healthy, young women (27.5 ± 1.1 y) of mixed ethnicity (5 Black or African-
51 American, 8 White, 1 American Indian/Alaska Native; 1 Hispanic/13 non-Hispanic) initiated the
52 study (Figure 1A and Table 1). Each was treated for four weeks with daily oral doses of 100 mg
53 mirabegron (Figure 1B). This dosage is higher than the maximum approved dosage (50 mg
54 daily) and was chosen because it was more likely to stimulate BAT (7). By Day 14 of treatment,
55 we presumed that the subjects' β 3-AR's were being stimulated continuously, as trough plasma
56 concentrations of mirabegron were nearly at the K_i of 55 nM (10): 40.3 ± 5.0 and 45.2 ± 4.5 nM
57 at Days 14 and 28, respectively (Figure 2 and Supplemental Table 1). At the completion of the
58 trial (Day 28), there were no changes in weight, fat mass, fat-free mass, or reported food intake
59 (Table 1).

60 The prespecified primary endpoint, the subjects' detectable BAT metabolic activity as
61 measured via [^{18}F]-2-fluoro-D-2-deoxy-D-glucose (^{18}F -FDG) positron emission
62 tomography/computed tomography (PET/CT), significantly increased (Figure 3, A and B and
63 Supplemental Figure 1), median 195 to 473 mL*g/mL ($P = 0.039$). Similar proportional
64 increases were seen with BAT volume (Figure 3C), median 72 to 149 mL ($P = 0.036$), and
65 maximum metabolic activity (Figure 2D), median 10 to 29 g/mL ($P = 0.017$). The extent of
66 changes in BAT activity and volume were not the same across the group. The women who had
67 less BAT on Day 1 had larger increases than those who started with more ($R^2=0.65$ and 0.71 ,
68 respectively, for activity and volume, both $P < 0.001$)(Supplemental Figure 3, A and B). These
69 patterns suggest that chronic mirabegron treatment is particularly effective at increasing BAT
70 activity in subjects who had little BAT before treatment, but there may also be an upper
71 threshold in its efficacy. Of note, while daily outdoor temperatures have been found to affect the

72 activity of BAT in response to cold stimulation (11), no relationship was found between the
73 change in \log_{10} BAT activity vs change in mean outdoor temperature by linear regression
74 ($R^2=0.11$, $P = 0.35$).

75 The PET/CT imaging also allowed us to measure metabolic activities of other tissues that can
76 contribute to thermogenesis. In contrast to BAT, ^{18}F -FDG uptake in erector spinae skeletal
77 muscle was unchanged (-0.01 ± 0.05 g/mL, $P = 0.77$) and was lower in the dorsal-lumbar depot
78 of subcutaneous WAT (scWAT) (-0.15 ± 0.04 g/mL, $P = 0.006$) (Figure 3, E and F). The reason
79 for assessing scWAT glucose uptake in particular was to determine if there had been a detectable
80 increase in thermogenic adipocytes in this very large depot. Since we did not detect any increase
81 in muscle or scWAT activity, it suggests that the major targets of chronic exposure to a β_3 -AR
82 are the adipose depots previously identified (12) (Supplemental Figure 3).

83 Human thermogenic adipocytes can be from two distinct lineages: constitutive “brown” in
84 the cervical and supraclavicular regions and recruitable “beige/brite” adipocytes in the
85 supraclavicular and abdominal depots, as well as other, smaller sites (13-18). Without biopsies,
86 the current study could not directly distinguish between these two cell types or whether the
87 increased metabolic activity was due to hypertrophy or hyperplasia. Based on the wide
88 distribution of activation, it is likely that both brown and beige/brite adipocytes contributed to
89 the higher metabolic activity (19). The increase was not uniformly distributed, with the
90 mediastinal, paraspinal, and abdominal depots showing the largest gains (Supplemental Figure 4)
91 (7).

92 To evaluate how mirabegron impacted whole-body metabolism, we used a repeated measures
93 ANOVA to determine the effects of day of study, time, and their interaction, on resting energy
94 expenditure (REE)(Figure 4A and Supplemental Table 2). There was a significant effect of both

95 time of day ($P < 0.001$) and the interaction between day of study and time of day ($P = 0.001$):
96 the initial dose of mirabegron on Day 1 increased REE by 10.7% ($+6.4 \pm 1.2$ kcal/h, $P < 0.001$),
97 yet the Day 28 dose of mirabegron did not further increase REE above the Day 28 pre-dose
98 baseline ($0.8\% = 0.5 \pm 1.2$ kcal/h, $P = 0.70$). However, the baseline REE (at 08:00) on Day 28
99 was 5.8% higher than baseline REE prior to drug exposure on Day 1 ($+82$ kcal/d, $P = 0.01$).

100 The respiratory quotient (RQ) reflects substrate source. The acute dose of mirabegron on
101 both Day 1 and Day 28, lowered the RQ (-0.069 ± 0.007 and -0.051 ± 0.007 , respectively; both P
102 < 0.001) (Figure 4B and Supplemental Table 3), indicating a net increase in fat oxidation. In
103 contrast to the results with REE, the baseline RQ on Day 28 was not different from Day 1 ($P =$
104 0.15), and the P value for the interaction between day of study and time of day was higher ($P =$
105 0.06). These changes in REE and RQ were likely due to both prolonged fasting and mirabegron
106 itself, but the lack of a placebo group precludes us from determining the contributions from each.
107 We also measured the energy expenditure and RQ for the entire chamber stay, from evening until
108 the next afternoon, and saw no difference in either parameter: 74.4 ± 8.4 kcal/h to 75.0 ± 8.0
109 kcal/h ($P = 0.57$) and 0.850 ± 0.023 to 0.854 ± 0.025 ($P = 0.51$), respectively. There were also
110 no changes in total sleep time or sleep efficiency: 391.8 ± 76.6 minutes to 354.5 ± 65.3 minutes
111 ($P = 0.11$), and $89.8 \pm 8.0\%$ to $91.5 \pm 4.6\%$ ($P = 0.27$), respectively. In addition, average core
112 temperature was 0.11 ± 0.02 °C higher on Day 28 (Supplemental Figure 5).

113 A concern related to chronic treatment with adrenergic agonists is pathologic overstimulation
114 of the cardiovascular system. Here, resting heart rate (HR), systolic blood pressure (SBP), and
115 rate-pressure product (RPP), a correlate of myocardial oxygen consumption (20), all increased
116 acutely on Day 1 in response to mirabegron, and baselines were higher on Day 28 (Supplemental
117 Table 4). Given that there is no published evidence yet to support direct binding of mirabegron

118 to either the β 1-AR or β 2-AR, these findings lend further support to the mechanism whereby
119 mirabegron is taken up by sympathetic nerve terminals and then causes the release of
120 norepinephrine to bind to cardiac β 1-AR's (21). Such cardiovascular stimulation is similar to
121 what we previously reported at 200 mg in men (7, 22) and demonstrates why dosages higher than
122 50 mg are not used clinically for overactive bladder. There was a diurnal variation in the change
123 in HR such that mirabegron increased HR more overnight than when the subjects were awake
124 and moving: $+6.2 \pm 1.7$ bpm between 19:00-22:00 vs $+8.4 \pm 1.5$ bpm between 00:00-03:00 ($P <$
125 0.001). None of the changes in HR or RPP correlated with the changes in REE (both $P > 0.05$,
126 not shown). Per self-administered questionnaires, 1-2 subjects reported occasionally
127 experiencing some of the anticipated mild treatment-emergent adverse effects (23): palpitations,
128 headaches, bowel habit changes, and tachycardia during exercise; none of these effects were
129 higher than Grade 1. The dose of mirabegron on Day 28 did not increase these cardiovascular
130 parameters any further. The changes were not long-lasting: two weeks after stopping treatment,
131 plasma mirabegron was 5.4 ± 0.1 nM, and heart rates returned to values at screening
132 (Supplemental Figure 6). Mirabegron treatment had no effect on exercise tolerance, with no
133 change in the maximal oxygen uptake (VO_{2max}), maximum heart rate, or maximum wattage
134 achieved (Supplemental Figure 7, A-C). Chronic mirabegron treatment also did not lead to
135 changes in measures of liver stiffness, liver steatosis, or gallbladder volume (Supplemental
136 Figure 7, D-F).

137 The effects of acute and chronic mirabegron treatment on plasma metabolites and hormones
138 could be separated into three distinct patterns (Supplemental Table 5). Most metabolites
139 demonstrated (A) no effect or changes resulting from fasting, independent of mirabegron.
140 However, one subset showed (B) acute increases on Day 28 that were blunted compared to Day

141 1: non-esterified fatty acids (NEFA) and β -hydroxybutyrate. Plasma level increases of these
142 metabolites was likely due to β 3-AR stimulation of WAT. It remains to be determined whether
143 chronic mirabegron treatment led to reduced responsiveness by the WAT or if there was
144 increased consumption of the metabolites.

145 The final pattern (C) of metabolite changes in response to chronic mirabegron treatment has
146 the greatest potential to improve metabolic health. There were increased fasting levels of the
147 following: high-density lipoprotein (HDL) (+8%), ApoA1 (+12%), ApoE (+7%), total bile acids
148 (+49%), total GIP (+31%), and adiponectin (+35%). In addition, there was a reduction in the
149 ApoB100/ApoA1 ratio, a biomarker of cardiovascular risk (24). We found higher levels of both
150 total chenodeoxycholic acid (CDCA) (1003 ± 254 to 1641 ± 359 nM, $P = 0.02$) and the
151 unconjugated form (212 ± 64 to 542 ± 159 nM, $P = 0.02$), the latter of which may be able to
152 further boost BAT thermogenesis (25).

153 Without altering body weight, the initial clinical trials using non-FDA approved β 3-AR
154 agonists provided some evidence for improved glucose tolerance (8) and insulin sensitivity (9).
155 In addition, rodent studies showed that β 3-AR-mediated activation of WAT can increase
156 pancreatic β -cell insulin secretion (26-28). To assess both glucose metabolism and β -cell
157 function in our study using mirabegron, we performed frequently-sampled intravenous glucose
158 tolerance tests (FSIGT, Figure 5, A and B) and quantified metabolic parameters using Bergman's
159 Minimal Model (Supplemental Table 6) (29). Modeling showed that the parameters associated
160 with insulin sensitivity, insulin-independent glucose metabolism, and insulin secretion all
161 increased substantially (Figure 5, C-F). Whole body insulin sensitivity (S_I), reflecting insulin's
162 action to both stimulate glucose uptake and suppress endogenous glucose production, increased
163 by 36% ($P = 0.026$). While S_I includes insulin's actions to both stimulate glucose uptake and

164 suppress endogenous glucose production, the effects on tissue glucose uptake are dominant (30).
165 Glucose effectiveness (S_G), the ability of glucose to mediate its own net disappearance
166 independent of elevated insulin response, increased by 34% ($P = 0.002$).
167 Regarding β -cell function, the acute insulin response to glucose (AIR_G) increased by 37% (P
168 = 0.039). The Disposition Index (DI), an overall measure of the ability of β -cells to secrete
169 insulin when normalized to the degree of insulin resistance, increased by 82% ($P = 0.005$).
170 Despite the increases in both S_I and AIR_G , there was no relationship between the changes in
171 these two measures for each of the subjects ($P = 0.39$). The change in HOMA-IR, a measure of
172 insulin resistance (31) was not significant after chronic mirabegron treatment (0.09 ± 0.81 , $P =$
173 0.72).

174 **DISCUSSION**

175 The labyrinthine paths toward developing pharmacological activators of β 3-AR's and BAT
176 thermogenesis to treat human metabolic disease have much in common. Both have been
177 bolstered by decades of highly encouraging preclinical studies (4, 5, 8, 9), yet to date, neither has
178 achieved its goal. A major step forward for the β 3-AR was the recent approval of mirabegron,
179 the first highly selective agonist, to treat overactive bladder (23). A single dose of mirabegron
180 stimulates BAT glucose uptake (22), a marker of thermogenesis, along with increases in WAT
181 lipolysis, REE, and changes in plasma bile acids (7). In this study, we report the physiological
182 effects of chronic daily oral treatment with mirabegron. The numerous potentially beneficial
183 metabolic responses now require determining which are attributable directly to mirabegron and
184 which are downstream of the initial effects.

185 Chronic mirabegron treatment increased BAT metabolic activity, the primary endpoint, and
186 this approach now joins chronic cold exposure as another way to augment BAT thermogenesis
187 (32-34). Two distinct facets of our findings relate to where and in whom BAT increased. The
188 preferential amplification of the perirenal depots is particularly noteworthy because of the recent
189 identification there of unilocular, dormant brown adipocytes (35). These cells express the β 3-AR
190 at much higher levels than scWAT and respond to treatment with adrenergic agonists by
191 increasing their thermogenic capacity. In addition, these dormant cells have less sympathetic
192 innervation, which could make them comparatively more responsive to pharmacological
193 activation through the blood than through cold exposure, which relies on sympathetic neurons.
194 Additional studies are needed to validate this model and determine if it applies to the mediastinal
195 and paraspinal depots as well.

196 The favorable changes in multiple lipoproteins and bile acids may also be connected to BAT
197 activation. A potential mechanism comes from a series of recent studies in mice showing that
198 when BAT is stimulated chronically, it consumes triglyceride-rich lipoproteins and subsequently
199 generates HDL cholesterol. HDL is then taken up and converted in the liver to bile acids,
200 particularly via the alternative pathway that preferentially synthesizes CDCA (36-39). The
201 plasma bile acids then bind to farnesoid X receptor (FXR) and TGR5 receptors and exert a
202 combination of metabolically beneficial effects through the liver, intestine, microbiome, and
203 mononuclear phagocytic system, including the production of incretins such as GIP (40, 41).
204 Future studies are required to corroborate the mechanisms by which the observed changes in
205 lipoproteins, adipokines, and bile acids are achieved and to conclusively demonstrate if these
206 effects represent new, physiologically relevant roles for BAT in human metabolism.

207 Besides effects on BAT, HDL cholesterol, and bile acids, mirabegron also produced
208 substantial improvements in glucose and insulin metabolism. In context, the increases we
209 observed in S_G , S_I , AIR_G , and DI , between 30-90%, were generally in the range of interventions
210 associated with improvements in insulin sensitivity or pancreatic β -cell function: an acute dose
211 of iv GLP-1 (S_I +4-29%, AIR_G +48-66%) (42, 43); chronic metformin treatment in women with
212 polycystic ovary syndrome (S_G +30%, S_I +2.5%, AIR_G +43%, DI +72%) (44); 9-15 months after
213 bariatric surgery (S_I +116%, AIR_G -56%) (45); and six weeks of mild exercise training in healthy
214 adults (S_G +28%, S_I +32%) (46). The improvements in glucose metabolism with mirabegron
215 treatment were not associated with changes in either fasting glucose or insulin. Similarly, iv
216 GLP-1 (42, 43) and exercise (46) did not raise or lower either fasting glucose or insulin levels,
217 while metformin lowered fasting glucose (44). Therefore, preliminary evidence suggests that

218 mirabegron's effects on glucose metabolism, HDL cholesterol, and bile acids resemble those
219 achieved through mild exercise (47, 48).

220 As mentioned above, the changes in S_I and AIR_G were not correlated. This discordance may
221 have been because mirabegron likely affects insulin sensitivity and β -cell function via different
222 mechanisms that are not directly connected. One reason for significant improvements in S_I and
223 S_G , but not the HOMA-IR, may have been that the subjects here had near-normal HOMA-IR at
224 study initiation (1.75 ± 0.69), and HOMA-IR does not provide a precise estimate of peripheral
225 insulin action in this population (49). Any significant effects of mirabegron on glucose
226 metabolism would therefore likely be detected only when glucose homeostasis was strongly
227 perturbed, such as in the setting of the FSIGT (50, 51).

228 How mirabegron improved glucose metabolism is not known. Contributions could have
229 been from the higher plasma adiponectin (52), a WAT-derived adipokine that is associated with
230 higher insulin sensitivity in skeletal muscle (53) and liver (54). The elevated levels of the
231 incretin GIP can also improve glucose-stimulated insulin secretion (55). A third, parallel
232 mechanism may involve the β -cells themselves. While we did not detect β_3 -AR mRNA in
233 human islets (data not shown), there is evidence that WAT lipolysis (26, 27, 56) followed by
234 activation of β -cell fatty acid receptor GPR40, can stimulate insulin release (57). In summary,
235 beneficial metabolic changes caused by chronic mirabegron treatment may come from
236 stimulation of the β_3 -AR on human BAT and WAT.

237 These findings must be considered in context of the principal limitations of this study: it
238 comprised a small group of young, healthy women with a narrow BMI range of diverse ethnicity,
239 and each was treated with active drug and served as her own control. Future studies are needed
240 using placebo controls in order to better determine whether the changes in BAT and other

241 physiological markers are dependent on mirabegron and what the contribution of mirabegron
242 was to the changes seen vs time and day. In addition, studies are needed in other populations,
243 such as the elderly and patients with metabolic disease. Also, while the FSIGT is a useful tool
244 for initial inquiries into insulin sensitivity and β -cell function, further studies are required to
245 identify tissue sites of improved metabolism. Finally, mirabegron's beneficial effects were seen
246 at a dosage higher than approved by the FDA, so the outcomes here cannot yet be applied to
247 patients. In particular, the elevations in HR, SBP, and myocardial oxygen consumption with this
248 dosage of mirabegron may confer too great a cardiovascular risk for clinical treatment of
249 metabolic dysfunction in obese patients. However, there are other β 3-AR agonists in late-stage
250 clinical trials that may have greater β 3/ β 1-AR selectivity (58, 59). Such drugs may improve
251 metabolism with an acceptable side effect profile.

252 In conclusion, we demonstrated that chronic treatment for four weeks with the β 3-AR agonist
253 mirabegron in healthy, young women with a range of BMI's led to increases in BAT metabolic
254 activity; REE; plasma HDL and associated lipoproteins; insulin sensitivity; and pancreatic β -cell
255 insulin secretion. These metabolic benefits occurred without changes in the subjects' weight, fat
256 mass, or lean body mass. Therefore, chronic activation of the β 3-AR may be an effective way to
257 treat metabolic disease.

258 **METHODS**

259 *Sample size calculation*

260 Our previous studies showed that BAT activity was not normally distributed; rather, it is
261 right skewed (7, 22). Thus, our sample size determination was based on \log_{10} BAT activity.
262 Since there were no published studies assessing the effects of mirabegron on \log_{10} BAT activity,
263 we used a similar cohort exposed to chronic cold exposure (32) that reported changes in \log_{10}
264 BAT volume of $+0.21 \pm 0.25$ mL. Since BAT volume correlates with BAT activity (12), we
265 then determined that a sample size of 14 female subjects was necessary to detect whether a
266 change in BAT metabolic activity was different from a null hypothesis of 0.00 with 80% power
267 using a paired Student's *t*-test with a significance level of 0.05 and a correlation (R) of 0.50.
268 Treatment was nonblinded for both staff and subjects.

269

270 *Subject Information and Protocol Design*

271 Inclusion criteria were the following: generally healthy women between the age 18-40 years.
272 Exclusion included were as described (<https://clinicaltrials.gov/ct2/show/NCT03049462>). Only
273 women were recruited because they were not included in our previous studies, which used a 200
274 mg mirabegron dose that can cause QT prolongation, values above 450 ms, in women but not
275 men (60). The protocol included a screening visit at which time we conducted a medical history
276 and physical examination, measured metabolites and hormones, and assessed the heart rhythm
277 via electrocardiogram (ECG); two study visits (Day 0-1 and Day 27-28); and a follow-up safety
278 visit to re-assess heart rate and rhythm, inquire about any adverse effects, and measure plasma
279 mirabegron, as described below and Figure 1A. In practice, "Day 28" was 28 ± 0.4 d after Day
280 0, and the follow-up safety visit was 16 ± 0.7 d after Day 28. Mean daily temperatures in

281 Bethesda, MD, for the 20 months of the study were obtained from the National Oceanic and
282 Atmospheric Administration (<https://www.ncdc.noaa.gov/cdo-web/search>) and are displayed in
283 Supplemental Figure 8 in relation to the subjects' individual study days. When a specific day's
284 temperature was not available, we used the day that was closest in time to the actual study day.

285 Twenty-two subjects enrolled; one was ineligible to participate; and seven either withdrew or
286 were lost to follow-up prior to initiation. All 14 subjects who initiated the study completed it.
287 Four of the 14 subjects reported travel outside of the Bethesda, MD, area during the study period
288 and could not be included in subsequent analyses related to outdoor temperature. Subjects were
289 asked to keep consistent weight-maintenance diets and exercise habits over the course of the
290 study. All 14 subjects who initiated the study completed it. There was high daily adherence to
291 medication administration, which was monitored using the Nomi Real-time medication
292 adherence technology (SMRxT) and also assessed by measuring trough concentrations of
293 mirabegron at two weeks and four weeks after study Day 1.

294

295 *Metabolic Testing: Day 0 & Day 27*

296 Healthy volunteers who passed screening were admitted to the Metabolic Clinical Research
297 Unit (MCRU) at the NIH Hatfield Clinical Research Center the evening before testing at the
298 initiation (Day 0) and completion (Day 27) of the study. The goal was to study all subjects on
299 Days 0/1 and Days 27/28 on the same day of their menstrual cycles. In practice, the difference in
300 days of the cycle between Days 0/1 and Day 27/28 was -0.6 ± 2.3 d. Of the 14 subjects, 12 were
301 studied within the first three weeks of their menstrual cycles. During the evenings prior to the
302 FSIPT and the BAT imaging, subjects ate a weight-maintenance, caffeine-free dinner of $716 \pm$
303 111 kcal with a macronutrient distribution of 55% carbohydrate, 15% protein, and 30% fat (61,

304 62). Prior to 12:00 am, they were provided a high-carbohydrate, high-protein snack that was 251
305 \pm 49 kcal. Inpatient rooms were kept at 24 °C, and subjects were asked to go to sleep at the same
306 time each night. Clothing was standardized during each metabolic chamber stay as described
307 (12).

308 Subjects fasted from 00:00 until completing testing later that day (Day 0/Day 27). Subjects
309 first underwent a frequently-sampled intravenous glucose tolerance test (FSIGT) from 08:00-
310 11:00. At time 0, participants received an intravenous bolus of glucose (0.3 g/kg body weight).
311 At 20 minutes, a bolus of insulin (0.03 U/kg body weight) was administered. Blood samples (~2
312 mL) for glucose and insulin were taken at -10, -1, 0, 1, 2, 3, 4, 5, 6, 7, 8, 10, 12, 14, 16, 20, 22,
313 23, 24, 25, 27, 30, 40, 50, 60, 70, 80, 90, 120, 150, and 180 minutes. Afterward, subjects met
314 with a dietician to review food intake records and collect anthropometric measures (neck, waist,
315 hip, arm, and leg circumference and length) in triplicate. Liver stiffness and steatosis were
316 assessed using vibration controlled transient elastography (VCTE) and continuous attenuation
317 parameter (CAP), respectively, with the Fibroscan device (Echosens, Waltham, MA) using the M
318 probe. Ten valid measurements were obtained, and the median result was used. Afterwards,
319 subjects ate an isocaloric lunch and underwent ECG testing. At 15:00, subjects performed a
320 VO_{2max} test to measure volitional fatigue on a cycle ergometer under a 15-20 W/min continuous
321 ramp protocol. At 17:00, a dual-energy X-ray absorptiometry (DXA) scan was performed
322 (iDXA, GE Healthcare, Madison WI). At 18:00, subjects entered the metabolic chamber.

323

324 *Quantification of Metabolic Activity, Physiological, and Clinical Measurements*

325 Subjects stayed in the metabolic chamber for 20 hours (18:00-14:00) during which energy
326 expenditure and respiratory quotient were measured via indirect calorimetry from oxygen

327 consumption and carbon dioxide production and ECG was recorded by a Holter monitor (Del
328 Mar-Reynolds, Irvine, CA, USA). Energy expenditure and RQ were calculated for the entire 20-
329 hour chamber stay, and the first and last 30 minutes were excluded in determining the overall
330 energy expenditure and RQ. At 18:00, they were provided an isocaloric dinner and snack; they
331 fasted from 00:00 until exiting the chamber the following day (Day 1/Day 28). Thirteen of 14
332 enrolled subjects completed the full overnight stay in the metabolic chambers. One subject
333 entered the metabolic chamber at 08:00 on Day 1/28 instead of 18:00 the prior night because of
334 scheduling constraints. Heart rate, and blood pressure, were determined as described (7, 63).
335 Core temperature was measured by the participant using a handheld infrared tympanic
336 thermometer (PRO4000, Braun, Melsungen, Germany).

337 The relative humidity of each chamber was controlled between 30-50%. The chamber's
338 temperature was set to 26 °C to ensure that BAT was not activated by cold exposure. While in
339 the chamber, subjects were asked to minimize their physical activity and stay awake other than
340 during their nightly sleep period. Sleep actigraphy was measured using triaxial accelerometers
341 (Actigraph GT3X+, Actigraph LLC, Pensacola, FL) worn on the wrist. We used the Cole-
342 Kripke algorithm implemented in ActiLife software (version 6.12.0) to detect time-in-bed, sleep
343 onset, and awakenings and recorded total minutes in bed, total sleep time, and sleep efficiency,
344 which is the ratio of the two (64).

345 Between 08:25-08:55 and 13:10-13:40, volunteers sat upright and still, without any physical
346 activity. These inactive periods provided motion-free data to calculate REE and resting heart
347 rate. Study subjects were administered 100 mg mirabegron at 09:00 (+0 minutes). Blood
348 samples used to measure blood metabolites were obtained 60 minutes prior to mirabegron dosing
349 (08:00) and then 60 minutes prior to exiting the metabolic chamber (13:00). Blood samples used

350 to test for plasma mirabegron concentrations were obtained at +0, +30, +60, +120, +180, +210,
351 +240, +270, +300, and +360 relative to the time of drug administration (09:00). Four hours after
352 mirabegron administration (13:00), volunteers were injected with a 185 MBq (5 mCi) bolus of
353 [¹⁸F]-2-fluoro-D-2-deoxy-D-glucose (FDG) for PET/CT scanning, after which subjects spent an
354 additional 60 minutes inside the chamber with limited physical activity to allow for uptake of the
355 radioactive tracer.

356 PET/CT images were acquired and analyzed as described (12, 65). In brief, PET/CT images
357 were reconstructed into image voxels of 1.45 × 1.45 × 1.5 mm for PET and of 0.98 × 0.98 × 1.5
358 mm for CT and uploaded into ImageJ for image processing (66). The PET/CT Viewer plug-in
359 with features customized for BAT quantification was used in each of the subsequent analyses.
360 Specific CT density ranges were used to identify fat (-300 to -10 HU) from air and other tissues.
361 ¹⁸F-FDG uptake (g/mL) in each PET image voxel was quantified as an SUV initially normalized
362 to the individual's lean body mass. Both PET SUV and CT HU criteria were met to identify
363 metabolically active adipose tissue.

364 BAT metabolic activity, defined as BAT volume multiplied by SUV mean, where SUV mean
365 is the average radioactivity concentration in BAT divided by injected FDG dose per body
366 weight. It, along with BAT volume; BAT, skeletal muscle, and scWAT SUV_{max}; and gallbladder
367 volume were quantified as previously described (7, 12, 65): one ROI was created on each axial
368 slice, avoiding regions that were not metabolically active fat in order to minimize false-positive
369 detection. ROI selection began at the slice corresponding to vertebra C3 and continued inferiorly
370 until the umbilicus. All axial ROIs were summed to calculate total body BAT volume and
371 activity, and SUVs were averaged to determine the SUV_{mean}. The study parameters have also

372 been summarized in Supplemental Tables 7-10 according to the Brown Adipose Reporting
373 Criteria in Imaging Studies (BARCIST 1.0) criteria (67).

374

375 *Measurement of Plasma Mirabegron and Individual Bile Acid Concentrations via UPLC-MS/MS*

376 Detection and quantification of mirabegron were achieved by ultra-performance liquid
377 chromatography - tandem mass spectrometry (UPLC-MS/MS) utilizing a Thermo Scientific
378 Vanquish UPLC with a Thermo Scientific Atlas triple quadrupole mass spectrometer as
379 described previously (7). Individual bile acid detection and quantification were achieved
380 utilizing a Thermo Scientific Vanquish UPLC with a Thermo Scientific Atlas triple quadrupole
381 mass spectrometer, heated electrospray ionization (HESI-II) in negative ion mode (2500 V).
382 Quantitation of bile acids and internal standard were based on the retention time and m/z .

383 Calibration stock solutions and internal standard $^2\text{H}_4$ -CDCA (10 ng/nL) were prepared in
384 MeOH and stored at 4 °C. 50 μL calibration stock standards were mixed with 50 μL H₂O and
385 150 μL internal standard for LC-MS analysis, plasma samples were prepared by protein
386 precipitation with 50 μL plasma mixed with 50 μL MeOH and 150 μL internal standard,
387 vortexed and then centrifuged at 4 °C, 14,000 rpm for 15 minutes. The supernatant was
388 transferred to an LC-MS vial. Injection volume was 2 μL injection.

389 High-performance liquid chromatography (HPLC) grade solvents and LC-MS modifiers
390 were purchased from Sigma-Aldrich (St. Louis, MO, USA). A Waters Acquity UPLC BEH C18,
391 2.1 x 100 mm, 1.7 μm column was maintained at 40 °C. Solvent A: H₂O, 5 mM NH₄OAc with
392 0.012% FA, and Solvent B: MeOH, 5 mM NH₄OAc with 0.012% FA. The flow rate was 400 μL
393 min^{-1} , the gradient was started 30% B from 0 min to 0.5min, increased to 95% B at 12 min,

394 maintained 95% B to 14 min, then returned to 30% B at 15 min to 18 min. Bile acids standards
395 were analyzed, and the calibration curve had a minimum $R^2 \geq 0.99$ with 1/x weighting.

396

397 *Measurement of Metabolites, Hormones, and Adipokines*

398 Glucose, insulin, non-esterified fatty acids (NEFA), glucagon, growth hormone, total T3, free
399 T4, TSH, ACTH, PTH, protein, creatine kinase, pyruvate, lactate, cortisol, norepinephrine,
400 epinephrine, and dopamine were measured by the NIH Department of Laboratory Medicine. For
401 epinephrine and dopamine concentrations that were below the assay detection limit, we imputed
402 the half-minimum value. Lipid profile (total cholesterol, high-density lipoprotein cholesterol
403 [HDL-C], low-density lipoprotein cholesterol [LDL-C], and triglycerides [TG]), were measured
404 using the Roche Cobas 6000 analyzer (Roche Diagnostics, Indianapolis, IN).

405 Metabolic proteins and hormones were measured at the NIDDK Clinical Core Lab. A
406 colorimetric assay kit was used to measure β -hydroxybutyrate (Cayman Chemical). Total bile
407 acids were measured in plasma using the NBT kit from Diazyme (Poway, CA). FGF-19, leptin,
408 and adiponectin were measured using Quantikine ELISA kits (R&D Systems). Active GLP-1,
409 active GIP, active Ghrelin, total PYY, total GIP, and FGF-21 were measured in plasma
410 containing DPP-IV and protease inhibitors from Sigma-Aldrich (St Louis, MO) using
411 immunoassay kits from Meso Scale Discovery (Rockville, MD). ApoA1, ApoE, ApoB100, and
412 ApoC3 were measured in plasma samples using the Milliplex (Billerica, MA) Human
413 Apolipoprotein Magnetic Bead Panel based on Luminex xMAP technology.

414

415 *Human Islet Studies*

416 Islets from previously non-diabetic or type 2 diabetic human cadaver donor pancreases were
417 obtained via the NIDDK-sponsored Integrated Islet Distribution Program (Duarte, CA) as
418 described (68). mRNA was extracted and quantified via qPCR as described (7).

419

420 *Statistical methods*

421 After completing the study in 14 subjects with detectable BAT, data were analyzed with JMP
422 13.0.0 software (SAS Institute, Inc.) and Graph Pad Prism 7.0 (GraphPad Software, Inc.). To
423 evaluate the primary endpoint, we used a paired Student's *t*-test on log-transformed data, which
424 was the prespecified analysis. All other paired comparisons were performed using either paired
425 Student's *t*-tests or repeated measures ANOVA, with the assumption that the underlying
426 distributions were normal. Simple linear regression was used to determine how the difference in
427 mean outdoor temperature between Day 1 and Day 28 affected \log_{10} BAT activity. All *P* values
428 are two-tailed, with statistical significance being *P* values ≤ 0.05 for comparisons associated with
429 the anthropometric, pharmacokinetic, bioenergetic, and glucometabolic measures. For the
430 behaviors of the 38 metabolites and hormones in Supplemental Table 5, the critical *P* value was
431 determined using a Benjamini-Hochberg false discovery rate $Q=0.25$ (69).

432

433 *Study approval*

434 This clinical trial was registered with ClinicalTrials.gov (NCT03049462) and has the FDA
435 Investigational New Drug registration number 116246. It was approved by the Human Studies
436 Institutional Review Board of the National Institute of Diabetes and Digestive and Kidney
437 Diseases (NIDDK) and the NIH Radiation Safety Committee. Healthy volunteers were recruited

438 by word of mouth or through the Patient Recruitment and Public Liaison Office of the Clinical
439 Center and provided written informed consent according to Declaration of Helsinki principles.

440 **Author Contributions**

441 AEO, JWJ, JDL, RJB, ASB, KYC, AMC were responsible for the experimental design. AEO,
442 JWJ, HC, PJW, AMC wrote the manuscript. AEO, JWJ, LAF, YF, NK, ASB, BPL, CMM, WD,
443 and PH quantified tissue metabolic activity. AEO, JWJ, JDL, RJB, SM, LAF, TC, KYC, and
444 AMC performed the physiological measurements. DK and YR assessed liver fat and stiffness.
445 HC, NBJ, and PJW measured plasma mirabegron and bile acid levels. JWJ, FP, M A, RNB,
446 AMC performed and analyzed the frequently sampled glucose tolerance tests. CC, ZAS
447 quantified human pancreatic β -cell mRNA expression. JWJ and AMC performed the
448 biostatistics. All authors contributed to editing the manuscript. AEO and JWJ contributed
449 equally to this work; AEO was primarily responsible for organizing and interpreting the clinical
450 data and is therefore listed first.

451

452 **Acknowledgements**

453 This work was supported by the Intramural Research Program of the National Institute of
454 Diabetes and Digestive and Kidney Diseases (NIDDK), DK075112, DK075116, DK071013, and
455 DK071014. We thank the excellent support provided by the NIH Metabolic Clinical Research
456 Unit nursing team; NIH Clinical Center Nutrition Department; NIDDK Clinical Laboratory Core
457 Lab; NIH Department of Laboratory Medicine; research pharmacy; and PET technologists. We
458 thank Douglas Rosing for being the independent internal data safety monitor. We offer additional
459 gratitude to Wouter van Marken Lichtenbelt for sharing his team's data so that we could perform
460 our sample size calculation; Sushil Rane and his lab for the gift of the human islets; Paul Wakim
461 and Sungyoung Auh for their biostatistical advice; Marc Reitman, Jack Yanovski, and Clifton
462 Bogardus for their discussions about the data and their implications; Anne Sumner, Sushil Rane,

463 and Gordon Weir for their guidance in interpreting the FSIGT data; and David Sacks and Jeff
464 Basilio for their advice in measuring tissue glycemia. We are especially thankful to our
465 volunteers for their commitment to our study.

466 Address correspondence to: Aaron M. Cypess, Diabetes, Endocrinology, and Obesity Branch,
467 Intramural Research Program, National Institute of Diabetes and Digestive and Kidney Diseases,
468 National Institutes of Health, Bethesda, MD 20892, USA. Phone: 301-435-9267; Email:
469 aaron.cypess@nih.gov

REFERENCES

- 470
471
- 472 1. Wang Y, Beydoun MA, Liang L, Caballero B, and Kumanyika SK. Will all Americans become
473 overweight or obese? estimating the progression and cost of the US obesity epidemic. *Obesity*
474 (*Silver Spring*). 2008;16(10):2323-2330.
- 475 2. Heymsfield SB, and Wadden TA. Mechanisms, Pathophysiology, and Management of Obesity. *N*
476 *Engl J Med*. 2017;376(15):1492.
- 477 3. American College of Cardiology/American Heart Association Task Force on Practice Guidelines
478 OEP. Expert Panel Report: Guidelines (2013) for the management of overweight and obesity in
479 adults. *Obesity (Silver Spring)*. 2014;22 Suppl 2:S41-410.
- 480 4. Liu X, Perusse F, and Bukowiecki LJ. Mechanisms of the antidiabetic effects of the beta 3-
481 adrenergic agonist CL-316243 in obese Zucker-ZDF rats. *Am J Physiol*. 1998;274(5):R1212-
482 1219.
- 483 5. Cannon B, and Nedergaard J. Brown adipose tissue: function and physiological significance.
484 *Physiol Rev*. 2004;84(1):277-359.
- 485 6. Arch JR. Challenges in beta(3)-Adrenoceptor Agonist Drug Development. *Ther Adv Endocrinol*
486 *Metab*. 2011;2(2):59-64.
- 487 7. Baskin AS, et al. Regulation of Human Adipose Tissue Activation, Gallbladder Size, and Bile
488 Acid Metabolism by a beta3-Adrenergic Receptor Agonist. *Diabetes*. 2018;67(10):2113-2125.
- 489 8. Cawthorne MA, Sennitt MV, Arch JR, and Smith SA. BRL 35135, a potent and selective atypical
490 beta-adrenoceptor agonist. *Am J Clin Nutr*. 1992;55(1 Suppl):252S-257S.
- 491 9. Weyer C, Tataranni PA, Snitker S, Danforth E, Jr., and Ravussin E. Increase in insulin action and
492 fat oxidation after treatment with CL 316,243, a highly selective beta3-adrenoceptor agonist in
493 humans. *Diabetes*. 1998;47(10):1555-1561.
- 494 10. Vrydag W, Alewijnse AE, and Michel MC. Do gene polymorphisms alone or in combination
495 affect the function of human beta3-adrenoceptors? *Br J Pharmacol*. 2009;156(1):127-134.
- 496 11. Senn JR, et al. Outdoor Temperature Influences Cold Induced Thermogenesis in Humans. *Front*
497 *Physiol*. 2018;9:1184.
- 498 12. Leitner BP, et al. Mapping of human brown adipose tissue in lean and obese young men. *Proc*
499 *Natl Acad Sci U S A*. 2017;114(32):8649-8654.
- 500 13. Wu J, et al. Beige adipocytes are a distinct type of thermogenic fat cell in mouse and human. *Cell*.
501 2012;150(2):366-376.

- 502 14. Sharp LZ, et al. Human BAT possesses molecular signatures that resemble beige/brite cells. *PLoS*
503 *One*. 2012;7(11):e49452.
- 504 15. Lidell ME, et al. Evidence for two types of brown adipose tissue in humans. *Nat Med*.
505 2013;19(5):631-634.
- 506 16. Cypess AM, et al. Anatomical localization, gene expression profiling and functional
507 characterization of adult human neck brown fat. *Nat Med*. 2013;19(5):635-639.
- 508 17. Jespersen NZ, et al. A classical brown adipose tissue mRNA signature partly overlaps with brite
509 in the supraclavicular region of adult humans. *Cell Metab*. 2013;17(5):798-805.
- 510 18. Sacks HS, et al. Adult epicardial fat exhibits beige features. *J Clin Endocrinol Metab*.
511 2013;98(9):E1448-1455.
- 512 19. Finlin BS, et al. Human adipose beiging in response to cold and mirabegron. *JCI Insight*.
513 2018;3(15).
- 514 20. Gobel FL, Norstrom LA, Nelson RR, Jorgensen CR, and Wang Y. The rate-pressure product as
515 an index of myocardial oxygen consumption during exercise in patients with angina pectoris.
516 *Circulation*. 1978;57(3):549-556.
- 517 21. Mo W, Michel MC, Lee XW, Kaumann AJ, and Molenaar P. The beta3 -adrenoceptor agonist
518 mirabegron increases human atrial force through beta1 -adrenoceptors: an indirect mechanism?
519 *Br J Pharmacol*. 2017;174(16):2706-2715.
- 520 22. Cypess AM, et al. Activation of human brown adipose tissue by a beta3-adrenergic receptor
521 agonist. *Cell Metab*. 2015;21(1):33-38.
- 522 23. Sacco E, and Bientinesi R. Mirabegron: a review of recent data and its prospects in the
523 management of overactive bladder. *Ther Adv Urol*. 2012;4(6):315-324.
- 524 24. Sandhu PK, et al. Lipoprotein Biomarkers and Risk of Cardiovascular Disease: A Laboratory
525 Medicine Best Practices (LMBP) Systematic Review. *J Appl Lab Med*. 2016;1(2):214-229.
- 526 25. Broeders EP, et al. The Bile Acid Chenodeoxycholic Acid Increases Human Brown Adipose
527 Tissue Activity. *Cell Metab*. 2015;22(3):418-426.
- 528 26. Grujic D, et al. Beta3-adrenergic receptors on white and brown adipocytes mediate beta3-
529 selective agonist-induced effects on energy expenditure, insulin secretion, and food intake. A
530 study using transgenic and gene knockout mice. *J Biol Chem*. 1997;272(28):17686-17693.
- 531 27. Gavrilova O, Marcus-Samuels B, and Reitman ML. Lack of responses to a beta3-adrenergic
532 agonist in lipotrophic A-ZIP/F-1 mice. *Diabetes*. 2000;49(11):1910-1916.

- 533 28. Heine M, et al. Lipolysis Triggers a Systemic Insulin Response Essential for Efficient Energy
534 Replenishment of Activated Brown Adipose Tissue in Mice. *Cell Metab.* 2018;28(4):644-655
535 e644.
- 536 29. Boston RC, Stefanovski D, Moate PJ, Sumner AE, Watanabe RM, and Bergman RN. MINMOD
537 Millennium: a computer program to calculate glucose effectiveness and insulin sensitivity from
538 the frequently sampled intravenous glucose tolerance test. *Diabetes Technol Ther.*
539 2003;5(6):1003-1015.
- 540 30. Bergman RN, Prager R, Volund A, and Olefsky JM. Equivalence of the insulin sensitivity index
541 in man derived by the minimal model method and the euglycemic glucose clamp. *J Clin Invest.*
542 1987;79(3):790-800.
- 543 31. Muniyappa R, Lee S, Chen H, and Quon MJ. Current approaches for assessing insulin sensitivity
544 and resistance in vivo: advantages, limitations, and appropriate usage. *Am J Physiol Endocrinol*
545 *Metab.* 2008;294(1):E15-26.
- 546 32. van der Lans AA, et al. Cold acclimation recruits human brown fat and increases nonshivering
547 thermogenesis. *J Clin Invest.* 2013;123(8):3395-3403.
- 548 33. Yoneshiro T, et al. Recruited brown adipose tissue as an antiobesity agent in humans. *J Clin*
549 *Invest.* 2013;123(8):3404-3408.
- 550 34. Hanssen MJ, et al. Short-term cold acclimation improves insulin sensitivity in patients with type 2
551 diabetes mellitus. *Nat Med.* 2015;21(8):863-865.
- 552 35. Jespersen NZ, et al. Heterogeneity in the perirenal region of humans suggests presence of
553 dormant brown adipose tissue that contains brown fat precursor cells. *Mol Metab.* 2019;24:30-43.
- 554 36. Bartelt A, et al. Brown adipose tissue activity controls triglyceride clearance. *Nat Med.*
555 2011;17(2):200-205.
- 556 37. Berbee JF, et al. Brown fat activation reduces hypercholesterolaemia and protects from
557 atherosclerosis development. *Nat Commun.* 2015;6:6356.
- 558 38. Dijk W, et al. ANGPTL4 mediates shuttling of lipid fuel to brown adipose tissue during sustained
559 cold exposure. *Elife.* 2015;4.
- 560 39. Worthmann A, et al. Cold-induced conversion of cholesterol to bile acids in mice shapes the gut
561 microbiome and promotes adaptive thermogenesis. *Nat Med.* 2017;23(7):839-849.
- 562 40. Chavez-Talavera O, Tailleux A, Lefebvre P, and Staels B. Bile Acid Control of Metabolism and
563 Inflammation in Obesity, Type 2 Diabetes, Dyslipidemia, and Nonalcoholic Fatty Liver Disease.
564 *Gastroenterology.* 2017;152(7):1679-1694 e1673.

- 565 41. Kuhre RE, et al. Bile acids are important direct and indirect regulators of the secretion of
566 appetite- and metabolism-regulating hormones from the gut and pancreas. *Mol Metab.*
567 2018;11:84-95.
- 568 42. Tan TM, et al. Combination of peptide YY3-36 with GLP-1(7-36) amide causes an increase in
569 first-phase insulin secretion after IV glucose. *J Clin Endocrinol Metab.* 2014;99(11):E2317-2324.
- 570 43. D'Alessio DA, Kahn SE, Leusner CR, and Ensink JW. Glucagon-like peptide 1 enhances
571 glucose tolerance both by stimulation of insulin release and by increasing insulin-independent
572 glucose disposal. *J Clin Invest.* 1994;93(5):2263-2266.
- 573 44. Pau CT, Keefe C, Duran J, and Welt CK. Metformin improves glucose effectiveness, not insulin
574 sensitivity: predicting treatment response in women with polycystic ovary syndrome in an open-
575 label, interventional study. *J Clin Endocrinol Metab.* 2014;99(5):1870-1878.
- 576 45. Vidal J, et al. Long-term effects of Roux-en-Y gastric bypass surgery on plasma glucagon-like
577 peptide-1 and islet function in morbidly obese subjects. *J Clin Endocrinol Metab.*
578 2009;94(3):884-891.
- 579 46. Nishida Y, et al. Effect of moderate exercise training on peripheral glucose effectiveness, insulin
580 sensitivity, and endogenous glucose production in healthy humans estimated by a two-
581 compartment-labeled minimal model. *Diabetes.* 2004;53(2):315-320.
- 582 47. Kodama S, et al. Effect of aerobic exercise training on serum levels of high-density lipoprotein
583 cholesterol: a meta-analysis. *Arch Intern Med.* 2007;167(10):999-1008.
- 584 48. Morville T, et al. Divergent effects of resistance and endurance exercise on plasma bile acids,
585 FGF19, and FGF21 in humans. *JCI Insight.* 2018;3(15).
- 586 49. Reaven GM. What do we learn from measurements of HOMA-IR? *Diabetologia.*
587 2013;56(8):1867-1868.
- 588 50. Wallace TM, Levy JC, and Matthews DR. Use and abuse of HOMA modeling. *Diabetes Care.*
589 2004;27(6):1487-1495.
- 590 51. Ader M, et al. Failure of homeostatic model assessment of insulin resistance to detect marked
591 diet-induced insulin resistance in dogs. *Diabetes.* 2014;63(6):1914-1919.
- 592 52. Kadowaki T, Yamauchi T, Kubota N, Hara K, Ueki K, and Tobe K. Adiponectin and adiponectin
593 receptors in insulin resistance, diabetes, and the metabolic syndrome. *J Clin Invest.*
594 2006;116(7):1784-1792.
- 595 53. Stefan N, et al. Plasma adiponectin concentration is associated with skeletal muscle insulin
596 receptor tyrosine phosphorylation, and low plasma concentration precedes a decrease in whole-
597 body insulin sensitivity in humans. *Diabetes.* 2002;51(6):1884-1888.

- 598 54. Stefan N, et al. Plasma adiponectin and endogenous glucose production in humans. *Diabetes*
599 *Care*. 2003;26(12):3315-3319.
- 600 55. Baggio LL, and Drucker DJ. Biology of incretins: GLP-1 and GIP. *Gastroenterology*.
601 2007;132(6):2131-2157.
- 602 56. MacPherson RE, Castellani L, Beaudoin MS, and Wright DC. Evidence for fatty acids mediating
603 CL 316,243-induced reductions in blood glucose in mice. *Am J Physiol Endocrinol Metab*.
604 2014;307(7):E563-570.
- 605 57. Pang Z, et al. GPR40 is partially required for insulin secretion following activation of beta3-
606 adrenergic receptors. *Mol Cell Endocrinol*. 2010;325(1-2):18-25.
- 607 58. Michel MC. How beta3 -adrenoceptor-selective is mirabegron? *Br J Pharmacol*.
608 2016;173(3):429-430.
- 609 59. Edmondson SD, et al. Discovery of Vibegron: A Potent and Selective beta3 Adrenergic Receptor
610 Agonist for the Treatment of Overactive Bladder. *J Med Chem*. 2016;59(2):609-623.
- 611 60. Malik M, et al. Proarrhythmic safety of repeat doses of mirabegron in healthy subjects: a
612 randomized, double-blind, placebo-, and active-controlled thorough QT study. *Clin Pharmacol*
613 *Ther*. 2012;92(6):696-706.
- 614 61. Mifflin MD, St Jeor ST, Hill LA, Scott BJ, Daugherty SA, and Koh YO. A new predictive
615 equation for resting energy expenditure in healthy individuals. *Am J Clin Nutr*. 1990;51(2):241-
616 247.
- 617 62. Malandrino N, et al. Visceral fat does not contribute to metabolic disease in lipodystrophy. *Obes*
618 *Sci Pract*. 2019;5(1):75-82.
- 619 63. Chen KY, et al. Brown fat activation mediates cold-induced thermogenesis in adult humans in
620 response to a mild decrease in ambient temperature. *J Clin Endocrinol Metab*. 2013;98(7):E1218-
621 1223.
- 622 64. Cole RJ, Kripke DF, Gruen W, Mullaney DJ, and Gillin JC. Automatic sleep/wake identification
623 from wrist activity. *Sleep*. 1992;15(5):461-469.
- 624 65. Kim K, et al. Whole Body and Regional Quantification of Active Human Brown Adipose Tissue
625 Using 18F-FDG PET/CT. *J Vis Exp*. 2019(146).
- 626 66. Barbaras L, Tal I, Palmer MR, Parker JA, and Kolodny GM. Shareware program for nuclear
627 medicine and PET/CT PACS display and processing. *AJR Am J Roentgenol*. 2007;188(6):W565-
628 568.

- 629 67. Chen KY, et al. Brown Adipose Reporting Criteria in Imaging Studies (BARCIST 1.0):
630 Recommendations for Standardized FDG-PET/CT Experiments in Humans. *Cell Metab.*
631 2016;24(2):210-222.
- 632 68. Kim SY, et al. Loss of Cyclin-dependent Kinase 2 in the Pancreas Links Primary beta-Cell
633 Dysfunction to Progressive Depletion of beta-Cell Mass and Diabetes. *J Biol Chem.*
634 2017;292(9):3841-3853.
- 635 69. Reiner A, Yekutieli D, and Benjamini Y. Identifying differentially expressed genes using false
636 discovery rate controlling procedures. *Bioinformatics.* 2003;19(3):368-375.
- 637 70. Du Bois D, and Du Bois EF. A formula to estimate the approximate surface area if height and
638 weight be known. 1916. *Nutrition.* 1989;5(5):303-311; discussion 312-303.
- 639

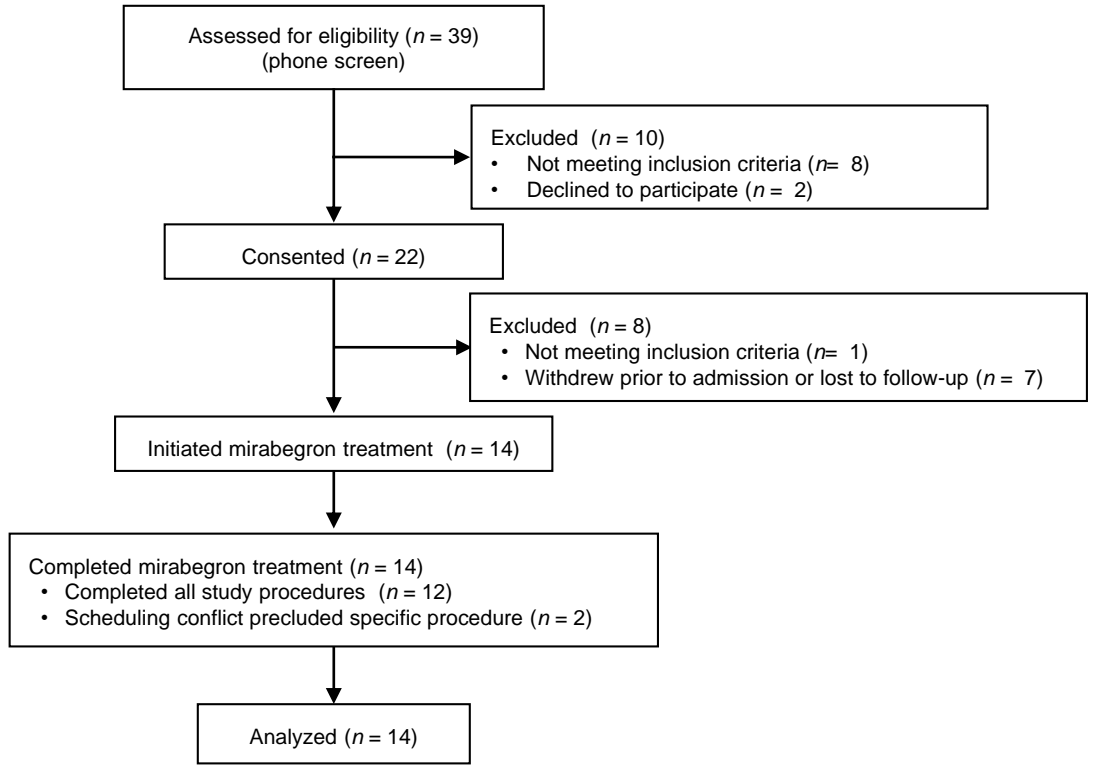
640 **Table 1. Anthropometric Values at Study Initiation and Completion**

Characteristic (Unit)	Day 0 Value ^A	Day 27 Value ^A	Paired <i>t</i> -test ^B
Height (cm)	163.3 ± 1.5	163.5 ± 1.5	0.36
Weight (kg)	67.5 ± 3.2	67.8 ± 3.3	0.40
Food Intake (kcal/d)	1938 ± 139	1854 ± 149	0.50
Body Mass Index (kg/m ²)	25.4 ± 1.2	25.4 ± 1.2	0.86
Body Surface Area (m ²)(70)	1.75 ± 0.04	1.75 ± 0.05	0.46
Body Fat (kg)	23.5 ± 2.1	23.6 ± 2.1	0.54
Percent Fat (%)	35.3 ± 1.6	35.2 ± 1.6	0.69
Fat-free Mass (kg)	43.9 ± 1.5	44.3 ± 1.5	0.24
Lean Mass (kg)	41.7 ± 1.4	41.9 ± 1.4	0.44
Percent Lean Mass (%)	62.4 ± 1.5	62.4 ± 1.5	0.72
Bone Mineral Content (kg)	2.40 ± 0.07	2.41 ± 0.07	0.21
^A Mean ± SEM			

641

Figure 1

A



B

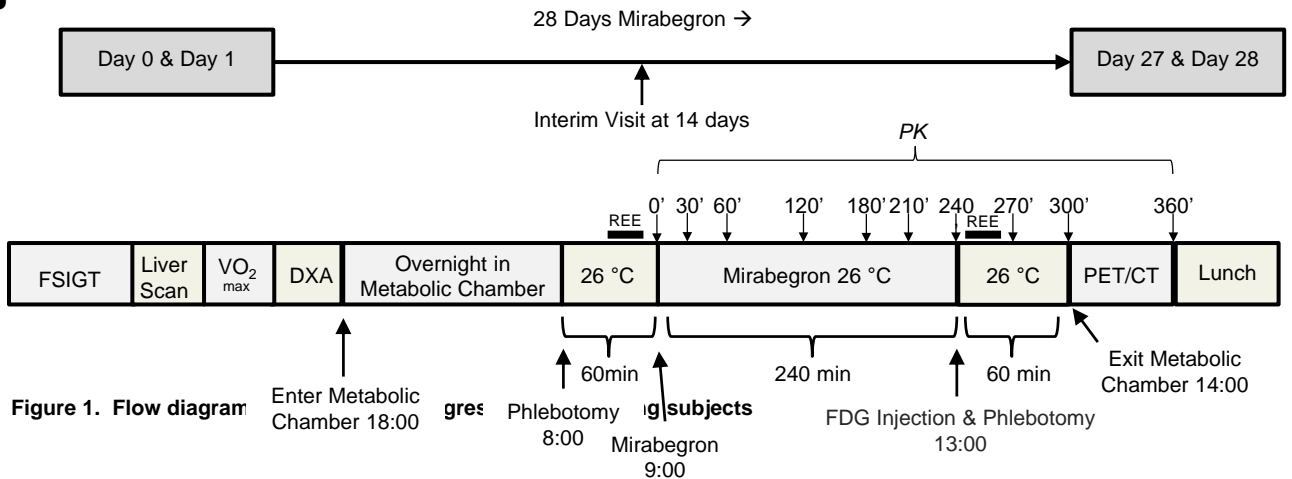


Figure 1. Flow diagram

Figure 1. Flow diagram and study design. (A) Flow diagram describing the numbers and disposition of study subjects. (B) Subjects underwent metabolic testing on Day 0/Day 27, consisting of a frequently-sampled intravenous glucose tolerance test (FSIGT), liver scan, exercise tolerance test (VO_{2max}), dual-energy X-ray absorptiometry (DXA), then entered the metabolic chamber at 18:00 and remained overnight and through 14:00 of Day 1/Day 28, after which they were transported to the PET/CT suite. Blood was drawn to measure metabolites before treatment on Day 1/Day 28 at 08:00 and then just prior to ¹⁸F-FDG administration in the chamber at 13:00. Mirabegron was administered at 09:00. The black bars above the diagrams refer to the 30-minute still periods at which resting energy expenditure (REE) was measured. The black arrows indicate the time points at which blood was drawn for pharmacokinetic measurements.

Figure 2

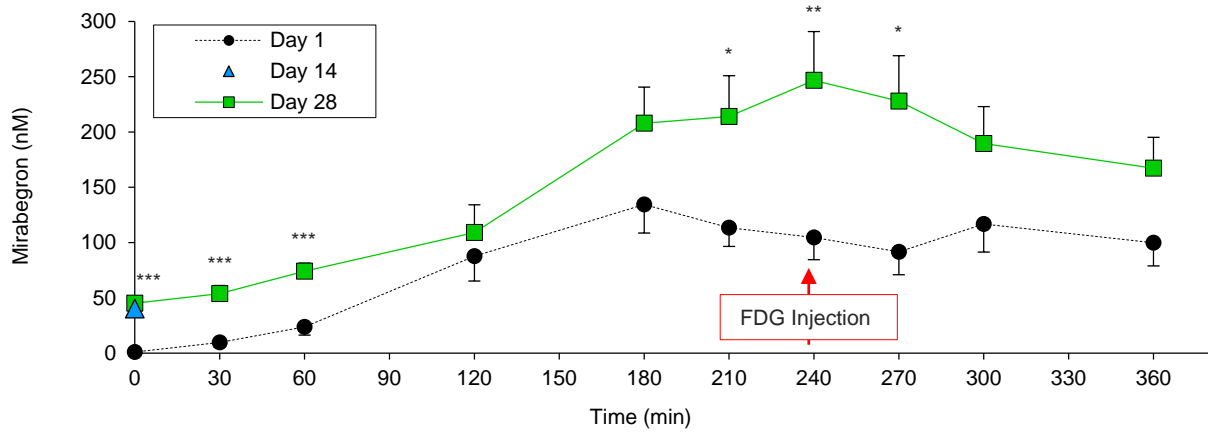


Figure 2. Mirabegron pharmacokinetics. Plasma concentration of mirabegron during Day 1 (black circles, dashed black line), interim visit Day 14 (blue triangle), and Day 28 (green squares, green line). The K_i of mirabegron is 55 nM. Values represent mean \pm SEM. $n = 12$. * indicates paired t -tests with $P < 0.05$; ** $P < 0.01$; *** $P < 0.001$.

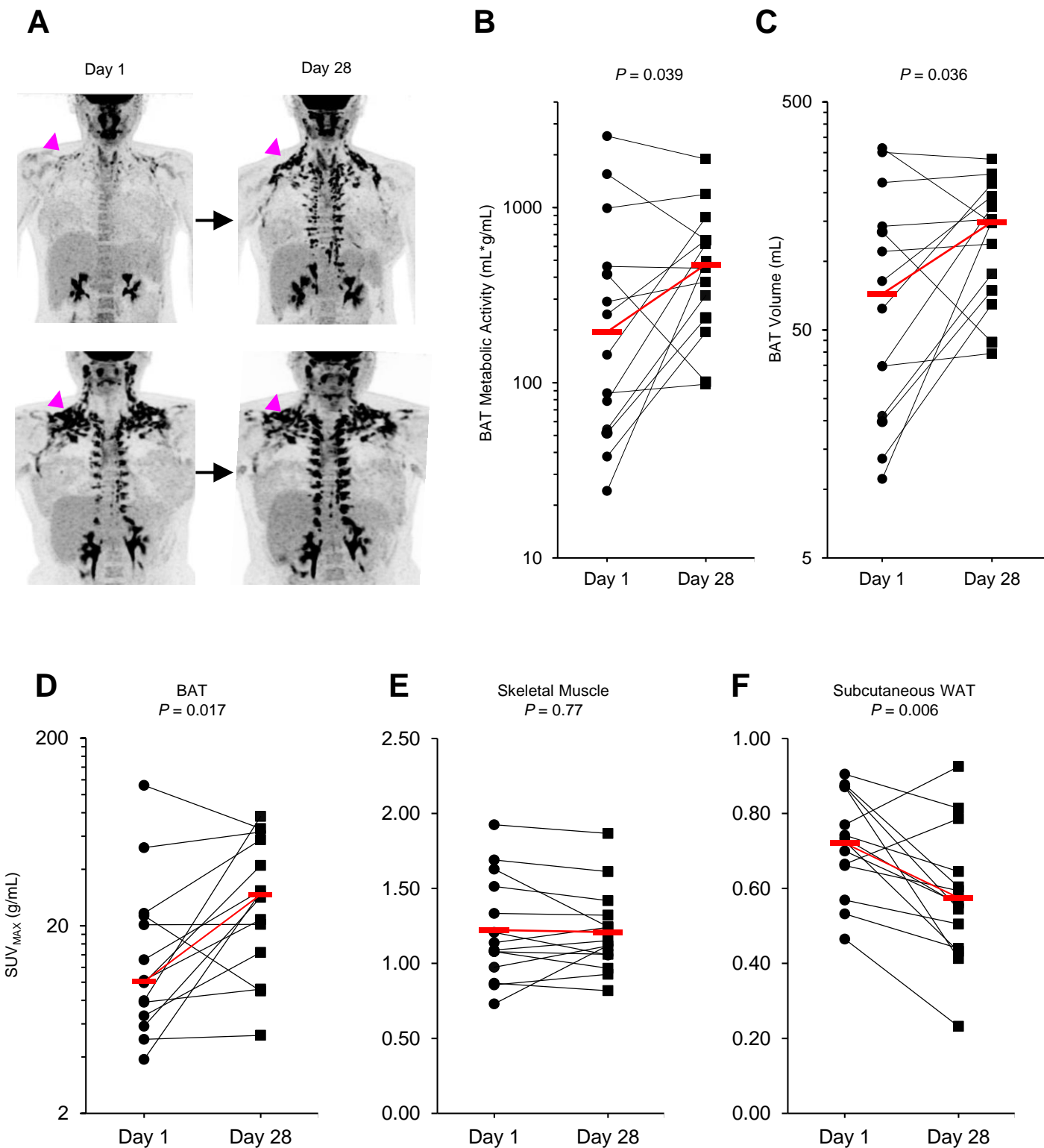
Figure 3

Figure 3. Effects of chronic mirabegron treatment on BAT, skeletal muscle, and subcutaneous WAT. (A) PET images on Day 1 and Day 28 in two representative subjects; magenta arrowheads point to the supraclavicular BAT depot with low (top) and high (bottom) initial BAT FDG-uptake after acute dose of mirabegron. Detectable BAT (B) metabolic activity and (C) volume in subjects on Day 1 (black circles) and Day 28 (black squares). Both y-axes are shown using a \log_{10} scale. P values are for the paired Student's t -test on the \log_{10} -transformed data, the prespecified analysis. SUV_{max} from PET scans taken on Day 1 and Day 28 of the subjects' (D) BAT, (E) erector spinae skeletal muscle, and (F) dorsolumbar subcutaneous WAT. Individual volume measured on Day 1 (black circles) and Day 28 (black squares); red bars represent group medians for BAT and means for skeletal muscle and WAT. P values are for the paired Student's t -tests. $n = 14$.

Figure 4

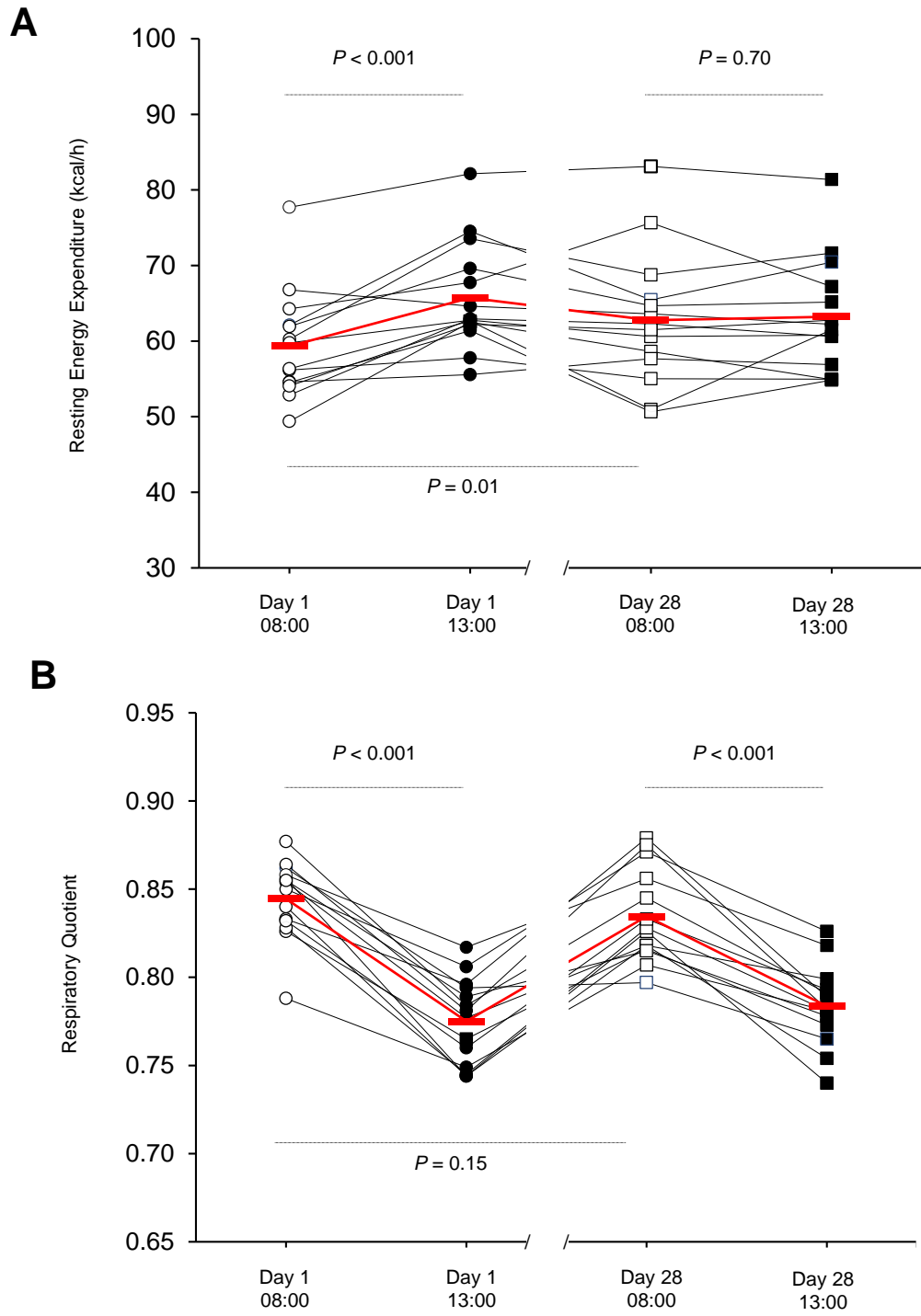


Figure 4. Effects of chronic mirabegron treatment on REE and RQ. Changes in (A) REE and (B) RQ in response to 100 mg oral mirabegron on Day 1 (circles) and Day 28 (squares) as measured in a metabolic chamber during 20-minute still periods at 08:00 (white circles and squares) and 13:00 (black circles and squares). Red bars represent group means. Repeated measures ANOVA was used to determine the effects of day of study, time, and their interaction. $n = 14$.

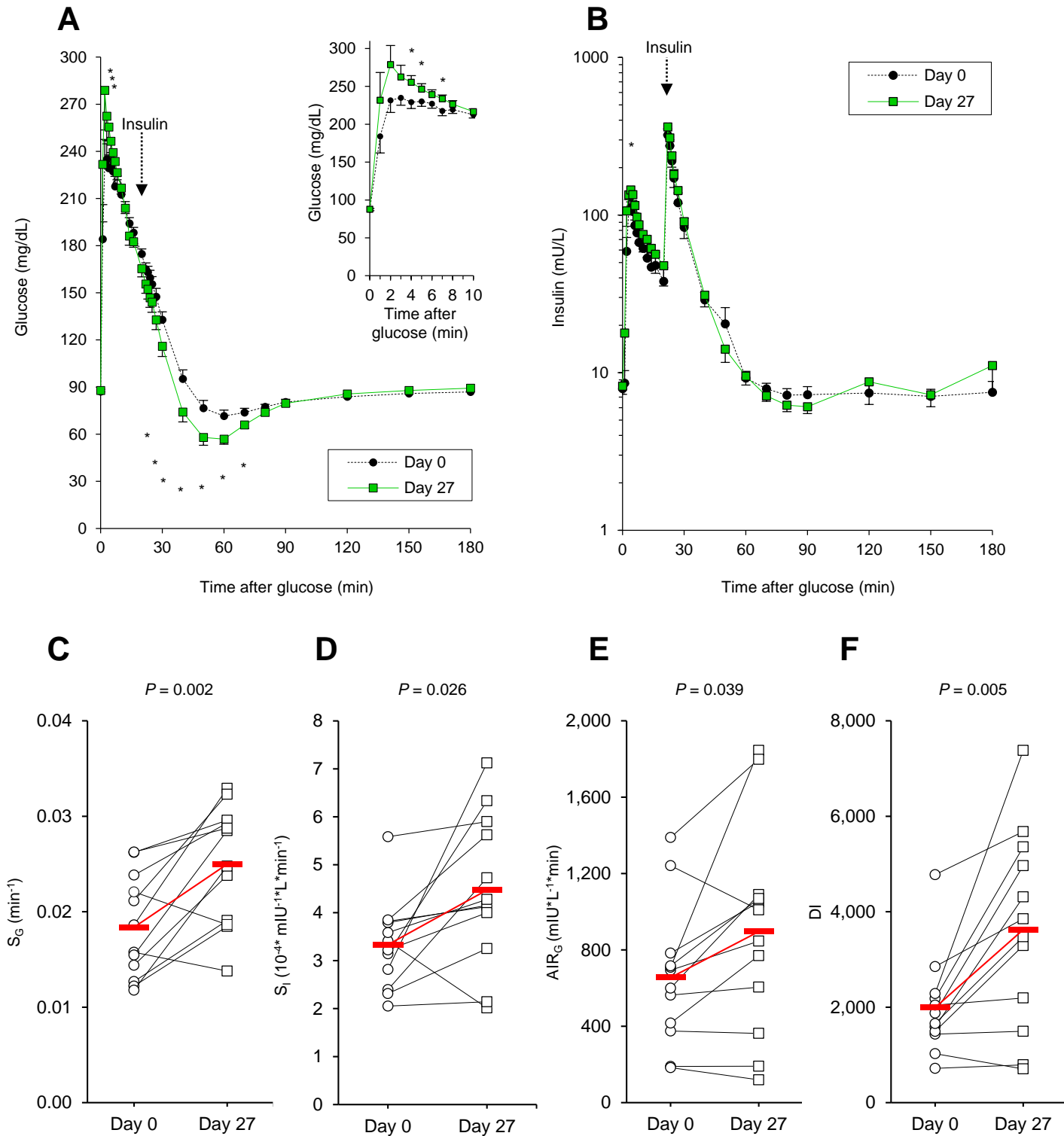
Figure 5

Figure 5. Frequently sampled intravenous glucose tolerance test outcomes. Plasma (A) glucose and (B) insulin responses during a frequently sampled intravenous glucose tolerance test on Day 0 (circles, black line) and Day 27 (squares, green line); error bars indicate SEM. The inset in (a) displays the levels from 0 to 10 minutes after injection of glucose. Individual changes in (C) glucose effectiveness (S_G), (D) whole-body insulin sensitivity index (S_I), (E) acute insulin response to glucose (AIR_G), and (F) the Disposition Index (DI). Red bars represent group means. Comparisons for each time point in (a) and (b) and between Day 0 (white circles) and Day 27 (white squares) in (c-f) were done with via paired Student's *t*-test, * $P < 0.05$. $n = 12$.